# Spectroscopy and Electrochemistry of the Covalent Pyridine-Cytochrome c Complex and a Pyridine-Induced, "Alkaline-like" Conformation

**Chunhai Fan,[†] Blake Gillespie,[‡] Guangming Wang,[†] Alan J. Heeger,*[,†,§] and Kevin W. Plaxco*[,‡]**

*Institute for Polymers and Organic Solids, and Department of Chemistry and Biochemistry and Interdepartmental Program in Biomolecular Science and Engineering, and Department of Physics and Department of Materials, University of California, Santa Barbara, Santa Barbara, California 93106*

*Received: May 17, 2002; In Final Form: August 5, 2002*

Spectroscopic studies demonstrate that at neutral pH and in the absence of specific pyridine binding, pyridine induces a conformational change in cytochrome c grossly similar to the alkaline-induced transition observed at high pH. This pyridine-induced conformational change has confounded previous efforts to characterize the electrochemistry of the covalent pyridine-cytochrome *c* complex. By employing cyclic voltammetry at a variety of time scales to characterize both kinetically and thermodynamically favored species, we demonstrate that, in the presence of pyridine, this pyridine-induced conformation coexists in a solution with native protein and a specific, covalent cytochrome c−pyridine complex. At low scan rates or in the presence of the nonbinding analogue 2-methyl pyridine, reduction of the pyridine-induced conformation is observed at potentials similar to those previously reported for the alkaline form populated at high pH in the absence of pyridine. At high scan rates and/or at slightly acidic pH the true redox reaction of the covalent pyridine-cytochrome c complex is resolved. Digital simulations of the voltammograms are quantitatively consistent with the proposed mechanisms, providing further support for the assigned redox rates and potentials.

## Introduction

Biological electron-transfer reactions play a critical role in almost every biochemical pathway. To optimize their function in vivo, evolution finely tunes the electrochemical properties of electron-transfer proteins by modulating the ligands and/or environment of the electron acceptor/donor.[1] In vitro, such tuning is similarly essential to the development and optimization of novel biocatalysts, biosensors and other biological devices.[2−4] Here, we explore in detail an example of electron-transfer tuning in the well-studied protein cytochrome c.

Cytochrome c (cyt c), a heme-containing protein participating in the mitochondrial respiratory chain, is perhaps the most extensively studied electron-transfer protein.[5,6] Due to its stability, ready availability, and well-characterized structure, it has served as a model for studies on electron-transfer complexes,[7−9] protein folding[10−12] and protein-polymer interactions.[13,14] Investigations on axial ligation of its heme iron have attracted special attention, in part because of its relationship to such biologically relevant processes as folding,[11,15] electron transfer,[16] and catalysis.[17] It has also been noted that coordination changes and structural rearrangements provide a means of coupling redox energy with "conformational energy" to modulate the protein's biological activity.[17,18]

In the native horse-heart protein, the redox properties of cytochrome c are defined in part by residues His18 and Met80, which serve as axial ligands to the heme iron.[19] A wide range of additional ligands, including both exogenous ligands such as cyanide,[20] azide,[21] $NH_3$,[22] imidazole,[23] or pyridine (Py) and endogenous ligands such as Lys73/79 (ref 24) or His26/33 (ref 25) have been shown capable of replacing the native Met80 ligand under some solvent conditions. The formation of complexes with these alternative ligands significantly modifies the structure, electron transfer properties, and, potentially, the biological function of the protein. For example, it is thought that intrinsic ligand substitution may occur during the formation of naturally occurring electron transfer complexes, which may modulate the protein's biologically relevant electron-transfer reactions.[26]

Among many studies on exogenous ligands, the interaction between cyt c and pyridine has received much recent interest.[24,27,28] Previous studies have demonstrated the formation of a specific cyt c−pyridine complex through ligand-binding, where pyridine replaces the native Met80 ligand and binds to the low-spin iron(III).[29,30] Recent nuclear magnetic resonance (NMR) investigations have revealed, however, that in addition to binding to form a covalent complex, pyridine can also induce a potentially significant conformational change in cyt c even in the absence of binding. This conformational change is reportedly similar to a novel conformation change normally observed at high pH and termed the "alkaline transition".[24]

The first identification of the alkaline conformation of cyt c occurred over 60 years ago,[31] when it was noted that above pH 9.5, the UV−vis spectra of the protein was significantly altered. Recent interest in this conformation has focused on its possible physiological relevance[32] and potential as a model for a late

* To whom correspondence should be addressed. E-mail: ajh@physics.ucsb.edu; kwp@chem.ucsb.edu.

[†] Institute for Polymers and Organic Solids, University of California, Santa Barbara.

[‡] Department of Chemistry and Biochemistry and Interdepartmental Program in Biomolecular Science and Engineering, University of California, Santa Barbara.

[§] Department of Physics and Department of Materials, University of California, Santa Barbara.

10.1021/jp0261307 CCC: $22.00 
Published on Web 10/03/2002

folding intermediate of the protein.[33] Extensive experimental studies, including NMR,[24] Raman spectroscopy,[34] electron spin resonance (ESR),[35] and electrochemistry[36] have been performed on the alkaline conformation and suggest that the transition involves replacement of the Met80-iron bond with a lysine acting as the new axial ligand.[35] Among the many lysines in cyt c, Lys73 and Lys79 are widely considered the most probable alternative ligands in the alkaline form of yeast cyt c.[35,37] Lys72, which is trimethylated in yeast cyt c, but remains unmethylated in the horse-heart protein, is also a possible ligand in the alkaline form of the latter. It has long been known that alkaline cyt c is significantly more difficult to reduce than the native conformation,[38−40] but its exact reduction potential was only recently resolved.[36]

Because pyridine both binds cyt c and, even in the absence of binding, produces a conformational change reportedly similar to the electrochemically significant alkaline transition, it has proven difficult to conclusively define the electrochemistry of the pyridine-bound protein. For example, one recent report on the electrochemistry of cyt c and pyridine apparently confused the processes of complex formation and the pyridine-induced conformational change.[28] Here, we unambiguously discriminate between these processes and assign the redox potentials of all of the relevant conformational states.

## Experimental Section

**Sample Preparation.** Horse-heart cyt c was purchased (Sigma, Type IV) and employed without further purification. The protein was dissolved in 25 mM of phosphate buffer of the appropriate pH, and the pH was checked upon the completion of the solution. Cyt c concentration was determined by absorbance (extinction coefficient $\epsilon = 106.1\ mM^{-1}\ cm^{-1}$ at 418 nm). Pyridine, deutero-pyridine, and 6-mecapto-1-hexanol were purchased from Sigma, 2-methyl pyridine (2-mpy), 3-methyl pyridine (3-mpy), and 4-methyl pyridine (4-mpy) were purchased from Aldrich, and guanidinium hydrochloride (GuHCl) was purchased from U. S. Biochemicals. All of the materials were employed without further purification.

**NMR Spectroscopy.** Horse-heart cyt c was dissolved in $D_2O$ and incubated at 60 °C for 6 h to exchange all of the labile protons. It was then lyophilized and stored at −20 °C. The NMR samples contained 5 mM cyt c, and the appropriate amounts of deutero-pyridine or 2-mpy. The pH values were not corrected for the isotope effect. NMR data were collected on a Bruker 500 M Hz spectrometer at 30 °C.

**Optical Spectroscopy.** Electronic absorption spectra were collected with a UV-2401PC spectrophotometer (Shimadzu). The spectra were recorded at room temperature and 10 $\mu$M cyt c. Circular dichroism (CD) measurements were performed with an AVIV circular dichroism spectrometer (AVIV Instruments, Inc., Model 202). The protein concentration was 12 $\mu$M. A 1.0 cm path-length quartz cuvette was employed and the temperature was controlled at 25 °C. Tryptophan fluorescence excited at 280 nm (slit-width 0.75 nm) was measured at 350 nm (slit-width 1.25 nm) at room temperature, using a 1.0 cm path-length quartz cuvette in a PTI fluorometer (Photon Technology International).

**Cyclic Voltammetry.** Cyclic Voltammetry (CV) was performed on 61 $\mu$M horse-heart cyt c using a CHI 603 workstation (CH Instruments) combined with a BAS C-3 stand. A gold working electrode, an Ag/AgCl/3 M NaCl reference electrode (BAS), and a platinum wire (BAS) were used as a normal three-electrode configuration. Potentials are reported against the Ag/AgCl/3 M NaCl reference electrode, unless specially mentioned. To convert potentials referenced to the Ag/AgCl/3 M NaCl to the standard hydrogen electrode (SHE), a 226 mV will be added.[41,42] The test solution was first thoroughly purged with argon. Then, a stream of argon was maintained above the protein solution to keep the solution anaerobic throughout the experiment. Background subtraction was conducted in some cases using Origin 6.0 (Microcal Software, Inc.) to remove non-Faradaic currents and improve signal clarity.[43]

The gold working electrode was either polycrystalline Au disk electrodes (1.6 mm diameters) from BAS or evaporated gold films. Essentially identical results were obtained with both electrodes. The preparation protocol for the gold electrodes was as follows: The Au disk electrode was polished to a mirror smoothness with aqueous slurries of successively finer diamond powder (from 12 $\mu$m to 1 $\mu$m) on nylon (rinsed with methanol) and finally with 0.03 $\mu$m alumina slurry on a polishing microcloth (rinsed with water), for at least 30 min. It was then rinsed thoroughly with nano-pure water (Milli-Q, Barnsted), and sonicated for 5 min. each in ethanol and water, respectively. The electrode was then electro-polished by potential cycling in 0.5 M KOH in the potential range of $-0.4 \sim -1.2$ V (at a scan rate of 100 mV/s) until the CV curve remained constant (>30 min). After rinsing, the Au electrode was immersed in a purged ethanol solution for ~20 min to remove absorbed oxygen. This clean Au electrode was then dried under argon and coated with a self-assembled monolayer (SAM) formed by immersion into a 1 mM ethanol solution of 6-mecapto-1-hexanol for 48 h. The modified electrode was washed with ethanol, dried under argon, and then employed in electrochemical measurements. The evaporated gold film was prepared by Electronic beam (Temescal VES-2550, Edwards). A 10 nm Ti adhesion layer was deposited on a pre-cleaned silicon surface followed by a 300 nm pure gold layer. The gold film was annealed at 200 °C for 1 h, followed by being slow cooled and plasma etched (PE II-A Plasma System, Technics; 300 Torr $O_2$/100 W/30 min.). The gold film was stored in a purged ethanol solution and dried under argon prior to SAM modification as described above.

**Digital Simulation.** Simulations of cyclic voltammograms were conducted using a powerful new electrochemical simulator, ESP 2.4 (by Dr. C. Nervi, nervi@lem.ch.unito.it). For electrochemical reactions, the formal potentials, diffusion coefficients, and apparent heterogeneous electron-transfer rates of each species were used as either inputs or simulated parameters. For chemical reactions, forward and backward homogeneous electron-transfer rates were simulated. The experimental parameters input for simulation are as follows: $E_{start} = 0.3$ V; $E_{switch} = -0.5$ V; $E_{end} = 0.3$ V; electrode area $= 0.02\ cm^2$; scan rates $= 0.025$, 0.1, and 0.5 V/s; redox potentials, diffusion coefficients, and apparent heterogeneous electron transfer rate constants are as experimentally determined; and the transfer coefficient, $\alpha$, is set at 0.5. Homogeneous reaction rate constants (as defined in Schemes 1 and 2), $k_{f,12}$, $k_{b,12}$, $k_{f,34}$, $k_{b,34}$, $k_{f,AC}$, $k_{b,AC}$, $k_{f,BD}$, and $k_{b,BD}$, are allowed to change during simulation.

## Results

Tang and co-workers have examined the effects of pyridine on cyt c using NMR spectroscopy.[27] Below pH 5.7, the NMR spectra of cyt c in the presence and absence of pyridine appear quite similar save for a resonance at 28.5 ppm that they assign to the 8-methyl group of the covalent pyridine cyt c complex (cyt c-Py). Above pH 5.7 they observe 2-D resonance consistent with the substitution of Met80 with a lysine residue in the presence of pyridine, a substitution also known to occur in the alkaline conformation.[27] They term the conformation thus

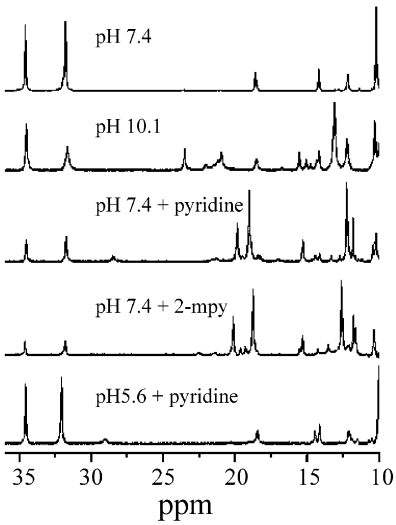


**Figure 1.** Downfield hyperfine-shifted region of the 1H NMR spectra of 5 mM horse-heart cyt c under the various solvent conditions explored here. An additional peak (at 28.5 ppm) corresponding to the cyt c-pyridine covalent complex arises in the presence of pyridine at pH 7.4. This peak is absent under alkaline conditions and in the presence of the nonbinding 2-mpy. In the presence of pyridine at pH 5.6, the conformation of cyt c is similar to the native form save for the appearance of the pyridine-complex peak at 28.5 ppm.

induced pycyt c. To clarify the relationship of cyt c-Py and pycyt c to each other and to the alkaline form of the protein, we have reproduced Tang and co-workers 1-D NMR studies (Figure 1) and complemented these with exhaustive optical spectroscopies and NMR studies employing a nonbinding pyridine analogue.

In the presence of pyridine at neutral pH, the hyperfine NMR spectrum of cyt c is altered significantly from that of the native protein, and includes a peak at 28.5 ppm previously assigned[27] to the covalent cyt c-Py complex (Figure 1). In the presence of pyridine at slightly acidic pH, by contrast, the NMR spectrum of cyt c closely resembles that of the native protein save for the additional peak at 28.5 ppm. In the presence of the pyridine analogue 2-methyl-pyridine (2-mpy) at neutral pH, by contrast, we observe that the NMR spectrum of cyt c resembles closely that of the pycyt c conformation save for the lack of a peak at 28.5 ppm. As 2-mpy does not bind cyt c,[24] this provides further support for Tang and co-workers' assignment of this peak to the covalent cyt c-Py complex.

Thus, pyridine apparently forms a covalent complex with cyt c and is capable of inducing a significant conformational change. The observation that the nonbinding analogue 2-mpy induces an identical conformational shift demonstrates that the formation of a covalent complex is not required. Given that spectra collected at neutral pH in the presence of pyridine indicate that a conformational change has occurred, and that the peak at 28.5 ppm is diagnostic of the covalent complex, it is apparent that both pycyt c and cyt c-Py may be populated under these conditions. By contrast, only cyt c-Py is present at low pH in the presence of pyridine, and only pycyt c is present at neutral pH in the presence of 2-mpy. These alternative conditions thus provide a means of deconvoluting the electrochemistry of the complex mixture produced by pyridine at neutral pH.

**Optical Spectroscopy.** Although pycyt c shares a Lys-iron ligand in common with the alkaline form of the protein, the 1-D NMR spectra of the two conformations indicate they are clearly not identical (Figure 1). To establish the degree to which alkaline cyt c and pycyt c are similar, we have conducted exhaustive optical spectroscopic characterization of the two as well as on the native and fully denatured states of the protein.

**Native Cyt c.** Absorbance spectra can provide telling evidence regarding identification of different conformations of cyt c.[5,38] Native cyt c at pH 7.4 exhibits a characteristic, intense Soret band at 409 nm. A relatively broad peak centered at 529 nm (Q-band) characteristic of the ferric state of cyt c is also observed (see the Supporting Information). Note that the spectrum exhibits a weak charge-transfer band at 695 nm that is unique for native Met80-Fe(III) ligation (Figure 2B inset).[5] These spectral features are clearly consistent with a well-folded, native protein in the ferric state.

The CD and fluorescence spectra of native cyt c are also indicative of a well-folded protein. The near-UV CD spectrum of native cyt c is characterized by a negative peak at about 285 nm (Figure 3B), demonstrating that the protein's aromatic side chains are well packed.[44−46] In the far-UV CD, an obvious negative peak at 218 nm is characteristic of proteins containing significant helical content (Figure 3A; solid line).[5,46] The Soret spectral region reports on interactions between the heme group and the peptide backbone.[47,48] As expected, obvious positive (at 393 nm) and negative (at 421 nm) "Cotton effects" are observed for the native protein (Figure 3C).[44,48] Trp59 is located proximal to the heme group in native cyt c, which quenches its fluorescence via energy transfer,[46,49] and thus, the native protein does not exhibit tryptophan fluorescence (Figure 4, solid line).

**Unfolded Cyt c.** The UV−vis, CD, and fluorescence spectra of cyt c unfolded in 5 M GuHCl are consistent with an unfolded, random-coil polypeptide. In the UV−vis spectrum, both the Soret band and the Q-band spectra shift to the blue (405 and 527 nm respectively), with a small increase in Soret intensity and a small decrease in Q-band intensity. The charge-transfer band at 695 nm is abolished, demonstrating that the native

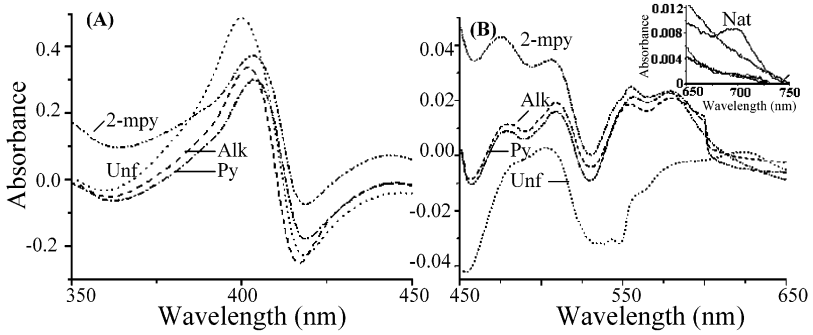


**Figure 2.** Difference spectra (from native, pH 7.4) of alkaline cyt c at pH 10.1 (dashed line, Alk); unfolded protein in the presence of 5.0 M GuHCl (dotted line, Unf); pyridine-induced state in the presence of 0.62 M pyridine (dash−dot line, Py) and 2-mpy-induced state in the presence of 0.62 M 2-methyl pyridine (dash−dot-dot line, 2-mpy). (A) Soret region (350−450 nm); (B) Q-band region (450−650 nm). Inset: UV−vis spectra of native cyt c at pH 7.4 (solid line, Nat), 650−750 nm. Conditions are as for Figure 1 except that pyridine and 2-mpy were at 0.62 M.

**TABLE 1: Redox Potentials of Various Conformers of Cyt c**

| | native form[a] | cyt c-ligand complex | | isomerized form | | conditions | | | |
|---|---|---|---|---|---|---|---|---|---|
| | ($E^{\circ\prime}$) | $E_{pc}$ | $E^{\circ\prime}$ | $E_{pc}$ | $E^{\circ\prime}$ | electrode | pH | $\mu$,[d] mM | ref |
| native cyt c | 0.069[b] | | | | | Au[e] | 7.4 | 25 | TW[f] |
| cyt c + pyridine | 0.067[b] | −0.205[c] | −0.120[c] | −0.365[b] | −0.286[c] | Au[e] | 7.4 | 25 | TW |
| cyt c + pyridine | 0.060[b] | −0.190[c] | −0.165[c] | | | Au[e] | 5.6 | 25 | TW |
| yeast iso-1 cyt c | 0.049 | | | −0.426 | −0.456 | PG[g] | 10.3 | 100 | 36 |
| cyt c + GuHCl | 0.038 | | | −0.446 | −0.393 | Au[h] | 6.0 | 100 | 15 |
| cyt c + 2-mpy | 0.063[b] | | | −0.392[b] | −0.382[c] | Au[e] | 7.4 | 25 | TW |
| cyt c + 3-mpy | 0.057[b] | −0.185[c] | ND[i] | −0.335[b] | −0.266[c] | Au[e] | 7.4 | 25 | TW |
| cyt c + 4-mpy | 0.054[b] | −0.174[c] | ND | −0.360[b] | −0.251[c] | Au[e] | 7.4 | 25 | TW |
| cyt c-pyridine complex | | | −0.159 | | | Au[j] | 7.0 | 25 | 28 |
| MP-8 + pyridine | | | −0.267 | | | GC[k] | 7.0 | 500 | 68 |
| cyt c + imidazole | 0.029 | ND | −0.325 | | | Au[h] | 7.0 | 100 | 54 |
| Phe82His mutant cyt c | 0.003 | | | −0.426 | −0.179 | Au[h] | 7.0 | 100 | 54 |
| *Desulfuromonas acetoxidans* cyt c[n] | −0.446 | | | | | PG[l] | 7.6 | 100 | 69 |
| cytochrome $b_5$[n] | −0.230 | | | | | Au[m] | 7.0 | 100 | 70 |

[a] Values are reported for horse heart cytochrome unless specially indicated. [b] Determined at low scan rates (<0.1 V/s). [c] Determined at high scan rates (>0.5 V/s). [d] $\mu$ indicates ionic strength. [e] Gold electrodes chemically modified with 6-mecapto-1-hexanol. [f] TW indicates this work. [g] Edge plane pyrolytic graphite electrodes. [h] Gold electrodes chemically modified with bis(4-pyridyl)disulfide. [i] ND stands for "not determined". [j] Gold electrodes modified with 4-pyridinyl-$CO_2$-$(CH_2)_6$−SH. [k] Glassy carbon electrodes. [l] PG electrodes modified with poly-L-lysine. [m] Gold mesh electrodes and determined with a spectroelectrochemical approach. [n] Heme proteins with natural bis-histidine axial coordination.

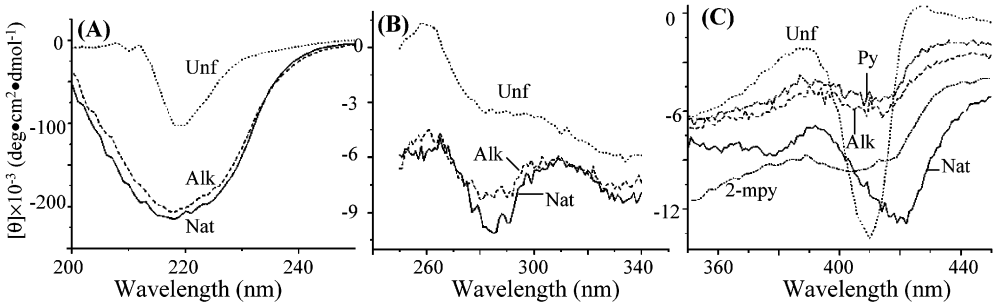


**Figure 3.** Far-UV (A), near-UV (B), and Soret (C) circular dichroism spectra of native cyt c (solid line, Nat); the alkaline form (dashed line, Alk); the unfolded protein (dotted line, Unf); the pyridine-induced state (dash−dot line, Py); the 2-mpy-induced state (dash−dot-dot line, 2-mpy). Conditions are as described in Figure 2.

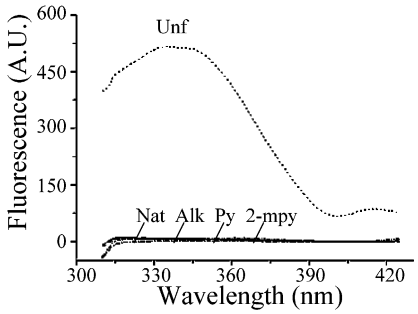


**Figure 4.** Unfolded cyt c exhibits obvious tryptophan fluorescence (dotted line, Unf), where as the native (solid line, Nat), alkaline (dashed line, Alk), pyridine-induced (dash−dot line, Py) and 2-mpy-induced forms (dash−dot-dot line, 2-mpy) lack tryptophan emission due to energy transfer between Trp59 and the heme, suggesting that all four conformations are approximately equally compact.

Met80-heme bond is broken (Figure 2B, inset, dotted line). The difference spectrum between unfolded and native cyt c provides a perhaps clearer indication of this change (Figure 2, dotted line): a positive band at 419 nm and a negative band at 400 nm (in the Soret region) demonstrate a shift in the heme ligation state.[50] In the range of 450−650 nm, both a large positive and a negative peak are observed, providing still more evidence that the environment of the heme is significantly altered.

CD and fluorescence spectroscopy also confirm that cyt c unfolds completely in 5 M GuHCl. The negative CD peak at 222 nm shifts to the red and decreases significantly in the presence of 5 M GuHCl, corresponding to an almost complete loss of secondary structure. Similarly, the loss of a negative CD peak at 285 nm corresponds to a complete loss of side chain packing (Figure 3B). Last, cyt c exhibits significant tryptophan emission in 5 M GuHCl, indicating that Trp59 is no longer in proximity to the heme group under these conditions.[50,51]

In the presence of 5 M GuHCl, the CD spectrum in the Soret region undergoes an obvious decrease in the intensity of the negative Cotton effect and a concomitant increase in that of the positive Cotton effect (Figure 3C), and the positions of both peaks shift (shown in Table 1 of the Supporting Information). The negative band has been proposed to be diagnostic of the Met80-Fe(III) bond.[52] Therefore, when combined with the loss of the 695 nm absorption, these results strongly suggest that ligand substitution and reorientation of the heme have occurred.[53]

**Alkaline Cyt c.** Optical spectroscopies confirm that the alkaline form of cyt c differs significantly from both native and unfolded cyt c. The UV−vis Soret band is blue-shifted and increases in intensity compared with that of the native protein, whereas the Q-band is red-shifted in comparison to the unfolded state (see the Supporting Information). The band at 695 nm is again invisible, which suggests that the native axial ligand Met80 is displaced (Figure 2B, inset). The difference spectrum of alkaline cyt c has two peaks similar to that of unfolded cyt c in the Soret region, with slight differences in the position and intensity. However, the spectral features in the range of 450−

650 nm are very different from those of the unfolded protein (Figure 2, and Table 1 in the Supporting Information).

The secondary structure of alkaline cyt c is relatively unperturbed; the intense negative peak at 218 nm in the far-UV CD spectra is only slightly attenuated and does not shift significantly (Figure 3A). Heme-group quenching of the tryptophan fluorescence spectrum in the alkaline form demonstrates that alkaline cyt c is compact (Figure 4). Moreover, the near-UV spectrum of alkaline cyt c also has the 285 nm peak observed in native form, albeit with some attenuation in intensity (Figure 3B). These features resemble the data in the previous report on CD spectra of molten globule states of cyt c, which is induced at low pH by high concentration of sodium chloride or sorbitol,[45] suggesting that the structure of alkaline cyt c may be at least somewhat more dynamic than that of the native protein. In the Soret CD, the magnitude of the negative Cotton effect is reduced, and the magnitude of the positive Cotton effect increased, indicating that the packing around the heme site has been disturbed (Figure 3C).

**Cyt c in the Presence of Pyridine and 2-Mpy.** In the presence of 0.62 M pyridine at neutral pH, the spectral features of cyt c are quite similar to those observed for the alkaline conformation. For example, both the Soret band and Q-bands of the UV−vis spectrum are nearly identical to those of the alkaline form. Similarly, the band at 695 nm is lost, indicating that the native Met80 is no longer the sixth ligand. This resemblance is even more readily observed in difference spectra (Figure 2); although differing from that of the unfolded protein, the spectrum of cyt c in the presence of pyridine is quite similar to that of the alkaline conformation. Tryptophan emission is also almost fully quenched under these conditions, indicating that, like the native and alkaline forms, the pyridine form is compact. Unfortunately, pyridine absorption is extensive across the entire UV region, preventing investigation of the effects of pyridine on either the far- or near-UV CD spectrum. Soret CD, however, clearly demonstrates that the pyridine-induced conformation closely resembles the alkaline form and that both are distinct from native and unfolded conformations (Figure 3C).

NMR spectroscopy suggests that although 2-mpy does not form a specific complex with cyt c, it does induce a conformation effectively identical to that populated in the presence of pyridine (Figure 1). Optical spectroscopy performed in the presence of 2-mpy confirms this similarity: although larger than those induced by pyridine, the spectral changes induced by 2-mpy closely resemble those of alkaline form and differ significantly from those observed upon complete unfolding. (Tables 1 and 2 in the Supporting Information).

**Cyclic Voltammetry.** CV provides a means of directly observing redox couples and the relative contributions of the reduction and oxidation currents to each couple. It is thus particularly useful in resolving multicomponent systems[54] and has proven of utility in investigations of conformational variations,[15,36,55−58] electron transfer between proteins,[59,60] and protein−ligand interactions.[61−64] However, due to either protein aggregation or denaturation at metallic surfaces, the direct electrochemistry (i.e., the direct electron transfer) of cyt c is prohibited at bare metal electrode surfaces.[60] To avoid this problem, a 6-mecapto-1-hexanol monolayer, a so-called electrochemical "promoter", is self-assembled on the gold surface to prevent direct contact of the protein. Critically, 6-mecapto-1-hexanol is electrochemically silent over the potential range of interest.

A pair of well-defined reduction and oxidation peaks are obtained for cyt c in phosphate buffer at pH 7.4 (Figure 5a).

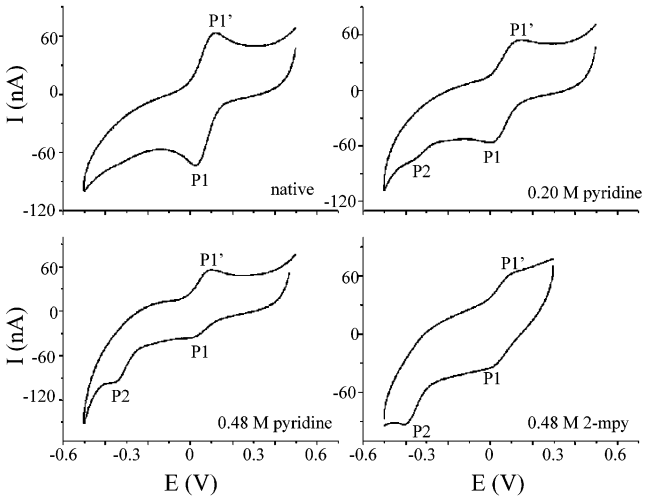


**Figure 5.** Cyclic voltammograms of cyt c at different concentrations of pyridine or 2-mpy at pH 7.4. The scan rate is 0.025 V/s and the potential is referenced to Ag/AgCl/3M NaCl. At this scan rate, only a pair of redox peaks, P1 and P1′, are observed for native cyt c, whereas an additional peak, P2, arises in the negative potential range in the presence of pyridine or 2-mpy.

Both the anodic ($I_{pa}$) and the cathodic ($I_{pc}$) peak currents are linearly proportional to the square root of scan rate up to rates of 1000 mV/s. The ratio of the two peak currents, $I_{pa}/I_{pc}$, is very close to 1.0 and is characteristic of a diffusion-controlled, quasi-reversible electrochemical process.[65] The apparent standard redox potential, $E^{\circ\prime}$, which is estimated from $E_{1/2}$ ($E_{1/2} = (E_{ox} + E_{red})/2$) to be 0.069 V, is quite close to previously reported values.[15] The diffusion coefficient, $D_0$, is estimated to be $1.10 \times 10^{-6}$ cm$^2$ s$^{-1}$, based on the Randles-Sevcik equation, and the apparent heterogeneous electron-transfer rate constant, $k_s$, is calculated to be 0.011 cm s$^{-1}$ (ref 66).

The presence of pyridine significantly alters the CV curve of cyt c (Figure 5). The redox couple corresponding to the reduction−oxidation of native cyt c remains (denoted as P1 and P1′ in Figure 5) and the $E^{\circ\prime}_{P1}$ of the native form does not change significantly; only a small decrease (-25 mV) is observed, possibly due to a pyridine-induced decreased dielectric constant[67] (see the Supporting Information). The $D_0$ is estimated to be $\sim 0.6 \times 10^{-6}$ cm$^2$ s$^{-1}$, a little lower than that in the absence of pyridine. The apparent heterogeneous electron-transfer rate constant, $k_s$, exhibits a limited dependence on the concentration of pyridine. It sharply decreases at lower concentrations of pyridine, while increasing at higher concentration (see the Supporting Information). This observation is similar to previous report on cyt c in acetonitrile solutions, which at least partly arises due to changes in the dielectric constant of the solution.[67] Markedly, a new reduction peak, P2, appears at ca. −0.16 V, whereas with further addition of pyridine, the original reduction peak diminished gradually (Figure 5). The P2 peak does not have an oxidation counterpart at a scan rate of 0.025 V/s. When the scan rate is increased to above 0.5 V/s, however, the corresponding oxidation peak, P2′, appears (Figure 6a, see below for discussion). The $E^{\circ\prime}$ is estimated to be −0.286 V at high scan rates. $E^{\circ\prime}_{P2}$ remains nearly constant with the increase of pyridine concentration. $k_s$ is estimated to be $1.2 \times 10^{-3}$ cm s$^{-1}$.

The CV curve clearly demonstrates that, in addition to native cyt c, there exist two non-native forms of the protein under these solvent conditions (pyridine itself is electro-inactive in this potential region, data not shown). The distribution of these three forms as a function of pyridine concentration can be estimated from the relative changes in their respective peak currents

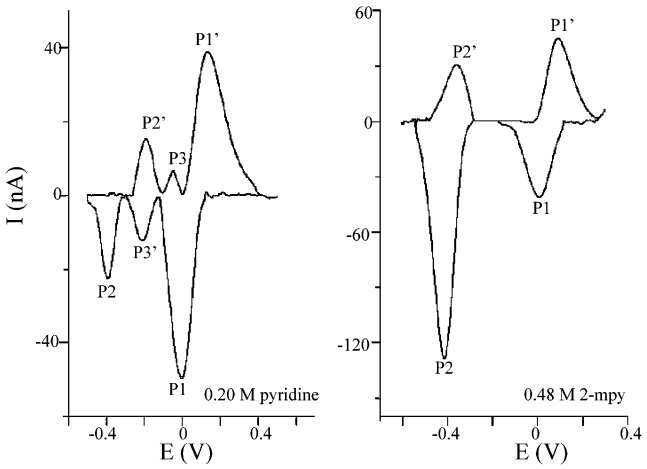


**Figure 6.** Background-subtracted cyclic voltammograms cyt c in a pH 7.4 phosphate solution in the presence of pyridine or 2-mpy. The scan rate is 0.5 V/s and the potential is referenced to Ag/AgCl/3M NaCl. At this scan rate, three pairs of redox peaks are observed in the presence of pyridine; they correspond to the reduction and oxidation of native cyt c (P1, P1′), pycyt c (P2, P2′), and the cyt c-Py complex (P3, P3′). In contrast, the peaks corresponding to the cyt c-Py complex are not observed in the presence of 2-mpy.

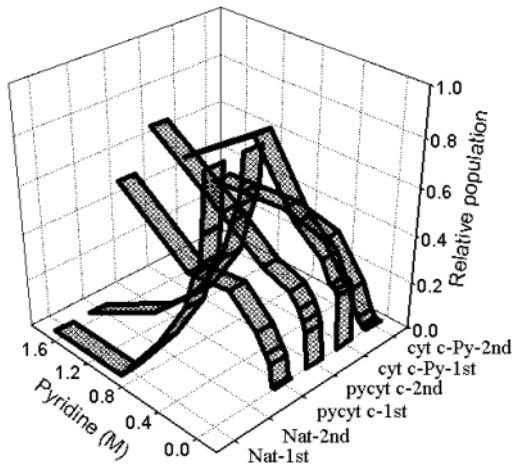


**Figure 7.** Plot of the relative population of three forms of cyt c verses the concentration of pyridine. "Nat" denotes the native form, "cyt c-Py" the cyt c-Py covalent complex and "pycyt c" the pycyt c conformation. first stands for the population of components in the time domain of the first cycle, whereas the second for those in the time domain of the second cycle cyclic voltammograms.

(Figure 7). It should be noted, however, that this estimation is not strictly quantitative because, in addition to relative abundances, peak currents are related to the electrochemical behavior of species under investigation.[57]

Which peak corresponds to cyt c-Py complex and which to the pycyt c form? Cyt c does not form a complex with 2-mpy, and therefore, this compound provides a means of discrimination between the two forms of the protein. In the presence of 2-mpy, cyt c exhibits only two CV redox pairs: the native reduction peak (P1) and an additional reduction peak (P2) consistent with the peak observed in pycyt c. The equivalent oxidation peak also appears at high scan rates (Figure 6b). From the midpoint potential we estimated that $E^{\circ\prime}$ is $-0.382$ V. The apparent heterogeneous electron-transfer rate of this redox couple, 0.010 cm $s^{-1}$, is much higher than the rate estimated in the presence of pyridine, demonstrating enhanced electrochemical reversibility in the presence of 2-mpy.

Although steric effects preclude the binding of 2-mpy, both 3-mpy and 4-mpy form complexes with cyt c,[27] consistent with this observation, both 3-mpy and 4-mpy produce similar CV features to that of pyridine, with only slight changes in peak position (Table 1). These results provide strong support for the assertion that peak P3 is the reduction peak of cyt c-Py covalent complex.

## Discussion

**Structural Features of pycyt c.** On the basis of NMR spectroscopic results, it has previously been reported that pyridine induces a conformation in cyt c analogous to the alkaline transition.[27] We have here confirmed these reports and furthered them with complementary optical spectroscopies. These additional spectroscopic studies demonstrate that pycyt c and the alkaline form of cyt c adopt grossly similar structures. In particular, the spectroscopic features indicative of the Met80-iron bond (both Soret CD and absorption at 695 nm) are completely absent in both pycyt c and alkaline cyt c, whereas other spectroscopic probes (tryptophan fluorescence, CD, and NMR) demonstrate that both species are compact and contain native-like secondary structure. Studies with 2-mpy at neutral pH and with pyridine at lower pH demonstrate that pyridine's ability to induce this conformational change does not require the formation of a covalent complex.

The origins of the pyridine-induced conformational change are far from clear. It has been suggested that organic cosolvents can induce molten globule states due to changes in the dielectric constant of the mixed solvent.[45,58,71] As the pyridine employed here significantly alter the dielectric constant of the solvent, such a mechanism may account for the increase in mobility required to produce the observed structural transition. Similarly, the reduced dielectric constant of pyridine solutions should reduce the p$K_a$ of lysine, thus increasing its affinity for the heme iron.

**Assignment of CV Peaks.** Yamamoto et al. have previously reported on the electrochemistry of cyt c in the presence of pyridine, producing CV curves essentially identical to those reported here.[28] (Figure 5b) Those authors assigned the new peak at ca. $-0.36$ V (P2) to the reduction of a covalent cyt c-Py complex in which pyridine binds to the heme iron in place of the native Met80. It is, however, quite possible that the reduction potential observed for pycyt c arises due to a pyridine-induced intramolecular rearrangement in which the native Met80-ligand is displaced by a lysine, rather than by the formation of a pyridine cyt-c covalent complex. This may be clarified by studies employing 2-mpy: as demonstrated by NMR here and elsewhere,[27] the steric effect of the additional methyl group prevents 2-mpy from binding the heme of cyt c. As the presence of 2-mpy cyt c produces a reduction peak similar to the P2 peak observed in the presence of pyridine (Figure 5d), it appears unlikely that this reduction peak is associated with the covalent complex. The data provided here suggest, instead, that this P2 corresponds to the reduction of a conformation quite similar to the alkaline form of cyt c, in which Lys79 or Lys73 replaces Met80. This assignment is supported by both spectroscopic evidence, indicating that pyridine induces an alkaline transition-like conformation in cyt c, and by the similarity in the electrochemical behavior of pycyt c and that previously reported for cyt c at alkaline pH.[36]

Additional evidence is provided by performing CV in a pH 5.6 solution containing both cyt c and pyridine. NMR reveals that, at this pH, pyridine does not induce an alkaline transition-like conformation; instead only native cyt c and the covalent cyt c-Py complex are observed. Under these conditions, a new redox couple, P3 and P3′, is evident at $\sim -0.161$ V, whereas

the peak corresponding to P2 is absent (Figure 8 and Table 1). P3 is thus undoubtedly the redox potential of the cyt c-Py complex. Further evidence in support of these assignments is derived from observations of 3-methyl pyridine (3-mpy) and 4-methyl pyridine (4-mpy): both form complexes with cyt c[27] and both produce peaks corresponding to P3 (Table 1).

Yamamoto has demonstrated that, when coordinated to a pyridine confined to the electrode surface via an inert spacer, cyt c produces a reversible current response at a potential close to that reported here for peak P3.[28] Although the authors assign this peak to a specific adsorption state of cyt c, we believe that it also corresponds to the cyt c-Py complex. This then provides further evidence in favor of our assignment of P3 to the redox reaction of the covalent cyt c-Py complex as, in these experiments, pyridine is absent from the bulk solution and thus cannot induce the pycyt c transition. It has also been shown that the pyridine bound heme-octapeptide (known as microperoxidase-8, MP-8) produces a reduction potential of −0.267 V, again supporting our assignment of P3 to the cyt c-Py complex.[68]

Although the redox couple of cyt c-Py complex (P3 and P3′) observed in acidic solutions is lost at a scan rate of 0.1 V/s at neutral pH, it is observed at neutral pH at a faster scan rates (> 0.5 V/s) or in the presence of relatively high concentration of pyridine (> 0.5 M). For example, at high scan rates a reduction peak arises at ca. −0.386 V, corresponding closely to the P3 peak observed in acidic solutions (Figure 6). This suggests that under these conditions, pyridine binding is kinetically, but not thermodynamically, favored.

**Mechanisms for Electrochemical and Coupled Chemical Processes.** The electrochemical process described here involves two parts: the formation of cyt c-Py complex (P3, P3′) and transition to pycyt c (P2, P2′). That the anodic peak currents for P3′ are lower than the cathodic peak currents for P3 at the pH employed, and the increased ratio, $I_{pa}/I_{pc}$, with increasing of scan rates (data not shown) suggest an "EC" reaction mechanism where a heterogeneous electron-transfer reaction occurring at the electrode surface (E) is coupled with a chemical reaction in solution (C).[65,72] Because nitrogen compounds bind feric cyt c more avidly than they bind ferrous cyt c,[73] at slow scan rates pyridine has sufficient time to dissociate from the ferrous heme after the ferric cyt c-Py complex is reduced. Thus, reoxidation of the ferrous cyt c-Py is not observed. At higher scan rates the dissociation reaction is incomplete, thus reoxidation of the unstable intermediate ferrous cyt c-Py can be monitored. These data reveal an electrochemically regulated process of electron transfer-related binding-dissociation.[61] This process is displayed in a similar scheme (Scheme 1)[63,74]

$$\text{cyt c(III)} + \text{Py} \underset{k_{b,12}}{\overset{k_{f,12}}{\rightleftharpoons}} \text{cyt c(III)-Py}$$

$$\text{cyt c(III)}\cdot\text{Py} + e \overset{E^{\circ\prime}_{P3}}{\rightleftharpoons} \text{cyt c(II)-Py}$$

$$\text{cyt c(III)}\cdot\text{Py} \underset{k_{b,34}}{\overset{k_{f,34}}{\rightleftharpoons}} \text{cyt c(II)-Py}$$

Here, $E^{\circ\prime}_{P3}$ represents the redox potential of cyt c-Py complex, $k_{f,12}$ and $k_{b,12}$ are the forward and backward homogeneous reaction rate constants for pyridine binding to ferric cyt c, and $k_{f,34}$ and $k_{b,34}$ are the forward and backward homogeneous reaction rate constants for the pyridine binding to ferrous cyt c.

Ferrous cyt c is much more resistant to unfolding by either denaturants[15] or high pH[36] than is ferric cyt c. Similarly, at a pyridine concentration at which ferric cyt c undergoes the alkaline transition, ferrous cyt c retains its native ligation.

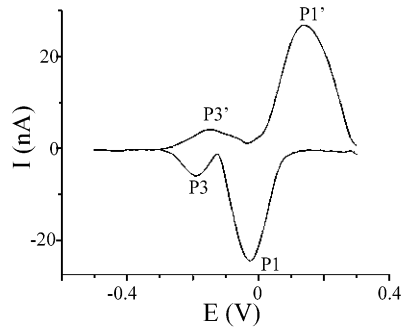


**Figure 8.** Background-subtracted cyclic voltammogram of cyt c in a pH 5.7 phosphate solution in the presence of 0.50 M pyridine. Under these conditions, two pairs of redox peaks are observed, corresponding to the reduction and oxidation of the native cyt c (P1, P1′) and the cyt c-Py complex (P3, P3′). By contrast, the peaks corresponding to the pycyt c (P2, P2′) are not observed. Further support of this assignment is provided by the observation that, in the presence of the nonbinding analogue 2-mpy, cyt c lacks peaks corresponding to P3 and P3′ (Figure 6). The scan rate is 0.1 V/s, and the potential is referenced to Ag/AgCl/3M NaCl.

Consistent with this, the P1 peak corresponding to the reduction of native ferric cyt c is significantly diminished and a peak P2 appears at a negative potential close to that of alkaline cyt c. This reduction produces an unstable lysine-ligated ferrous cyt c, which spontaneously converts to the native state through ligation substitution. Because of this, only the oxidation of native cyt c is observed when the potential scan is reversed (peak P1′) at low scan rates. If the potential scan is rapid enough to exceed the ligand substitution rate, then the oxidation of the transient ferrous pycyt c species can be captured (peak P2′). This process can be described with a square mechanism as follows (Scheme 2)

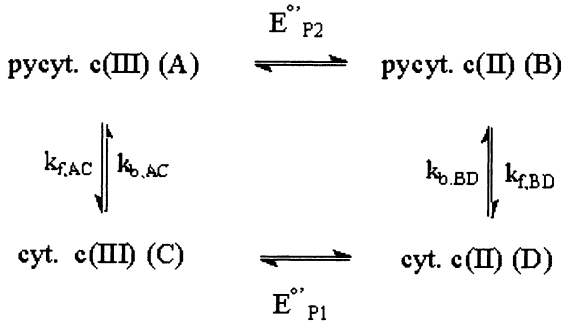


Here, $E^{\circ\prime}_{P2}$ and $E^{\circ\prime}_{P1}$ stand for the redox potentials of pycyt c and native cyt c, respectively, $k_{f,AC}$ and $k_{b,AC}$ are the forward and backward homogeneous reaction rate constants for the pyridine-induced transition of ferric cyt c, and $k_{f,BD}$ and $k_{b,BD}$ are the forward and backward homogeneous reaction rate constants for the pyridine-induced transition of ferrous cyt c.

**Evaluation of Mechanisms by Digital Simulation.** Digital simulation of a series of cyclic voltammograms at different scan rates was performed to further substantiate the above-mentioned mechanisms. The two processes, exogenous ligand binding and endogenous ligand substitution, are combined in the simulation. The initial concentrations of the various species were estimated from the experimentally obtained data (as in Figure 7). In all, seven species are involved, with three electrochemical reactions and four chemical reactions. Among them, the eight chemical reaction rate constants (forward and backward) are thermodynamically restricted. From the Nernst equation and Scheme 1, we obtain $E^{\circ\prime}_{P1} - E^{\circ\prime}_{P3} = 0.059\log(K_{12}/K_{34})$. Similarly, from

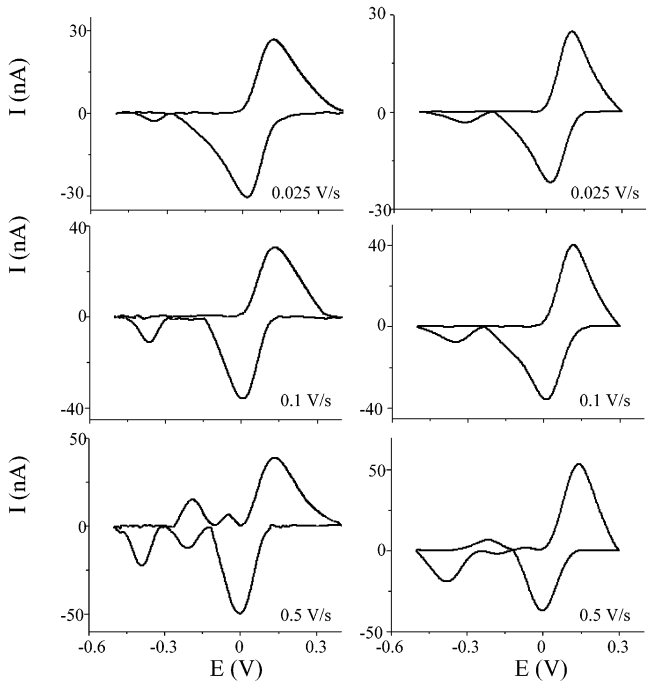


**Figure 9.** Observed (left) and simulated (right) background-subtracted cyclic voltammograms of cyt c in the presence of 0.20 M pyridine. The semiquantitative strongly supports the proposed electrochemical mechanism. Conditions are 25 mM, pH 7.4 phosphate solution and the potential is referenced to Ag/AgCl/3M NaCl.

the Nernst equation and Scheme 2, we obtain $E^{\circ\prime}_{P1} - E^{\circ\prime}_{P2} = 0.059\log(K_{AC}/K_{BD})$, where $K = k_f/k_b$.

The simulation equations and resulting parameters are as follows:

Electrochemical reactions

$$\text{Cyt c(III)} + e \leftrightarrow \text{cyt c(II)},\ E^{\circ\prime}_{P1} = 0.067\ \text{V},\ k_s = 1.0 \times 10^{-3}$$

$$\text{Pycyt c(III)} + e \leftrightarrow \text{pycyt c(II)},\ E^{\circ\prime}_{P2} = -0.286\ \text{V},\ k_s = 1.2 \times 10^{-3}$$

$$\text{Cyt c-Py(III)} + e \leftrightarrow \text{cyt c-Py(II)},\ E^{\circ\prime}_{P3} = -0.120\ \text{V},\ k_s = 7.0 \times 10^{-4}$$

Chemical reactions

$$\text{Cyt c(III)} + \text{Py} \leftrightarrow \text{Cyt c-Py(III)},\ k_{f,12} = 10,\ k_{b,12} = 6$$

$$\text{cyt c(II)} + \text{Py} \leftrightarrow \text{Cyt c-Py(II)},\ k_{f,34} = 3.5 \times 10^{-3},\ k_{b,34} = 3$$

$$\text{Cyt c(III)} \leftrightarrow \text{pycyt c(III)},\ k_{f,AC} = 0.01,\ k_{b,AC} = 1.0 \times 10^{-4}$$

$$\text{cyt c(II)} \leftrightarrow \text{Pycyt c (II)},\ k_{f,BD} = 1.0 \times 10^{-3},\ k_{b,BD} = 10$$

Given the large number of species and kinetic parameters involved in the model, the fact that the kinetic parameters were obtain by estimation, and the relatively poorly constrained potentials of peaks P3 and P3′, this model should not be expected to be in precise quantitative agreement with the observed CVs. Nevertheless, using this set of parameters, the simulated CVs have essentially all of the features observed in the experimental CVs (Figure 9) and thus strongly support the proposed mechanism. For example, changing $k_{b,BD}$ to 15 $s^{-1}$ or 5 $s^{-1}$ produces simulated waveforms quite distinct from those observed experimentally at one or more scan rates.

The reaction rate for ligand substitution, $k_{b,BD}$ is of relevance to the pyridine-induced transition as well as the folding of ferrous cyt c and provides further support for the proposed mechanism. The $k_{b,BD}$ reported ($\sim$10 $s^{-1}$) here coincides well with the 8.5 $s^{-1}$ value determined spectroscopically for alkaline, ferrous cyt c at pH 9 (ref 75). Histidine. The refolding of cyt c involves a ligand substitution from histidine which ligates heme in the unfolded protein[76] to Met80: this substitution acts as a kinetic trap that is the rate-limiting step in cyt c folding.[10,77] McLendon and co-workers studied the unfolding-folding of cyt c via an electrochemical approach.[15] However, they did not observe a reoxidation peak for unfolded cyt c at a scan rate as high as 1 V/s, implying that the refolding rate still exceeds this scan rate. Duplicating their work at a scan rate of 5 V/s we have successfully captured this transient process (data not shown), estimate $k_b$ to be about 18 $s^{-1}$ via a digital simulation approach and a square mechanism similar to that of Scheme 2. This simulation-derived value matches well with the value reported by Gray et al. using time-resolved absorption spectroscopy.[77] Consistent with this observation, Feinberg et al. estimated the $k_{f,BD}$ to be larger than 10 $s^{-1}$ via the study of a Phe82His variant of yeast iso-1-cyt c in which His82 acts as an alternative ligand.[54]

## Conclusions

With the above discussion, we arrive at a global interpretation of the electrochemistry of cyt c in the presence of pyridine. During the CV scan, there exists equilibrium between the solution and the electrode surface with the protein molecules in the solution diffusing to the electrode surface to undergo redox reactions. It is known that the three states—native ferric cyt c, ferric pycyt c, and ferric cyt c-Py complex—exist at neutral pH in the presence of pyridine. Under these conditions, there is competition between pyridine binding and the pyridine-induced conformational change. Because pyridine's affinity for heme iron is relatively low,[23] and the intrinsic ligands (Lys72/73/79) are entropically favored over exogenous ligands, the latter process—conformational change—predominates. Prior to the first potential scan, the distribution of these components in the bulk solution and at the electrode surface is essentially identical. When the scan proceeds from the positive potential, all three forms of ferric cyt c are gradually reduced to the corresponding ferrous forms at the electrode. Due to structural differences between ferric and ferrous cyt c, the latter disfavors either intrinsic ligand transition or pyridine binding. Thus, once ferrous cyt c is formed, the protein undergoes a structural rearrangement: either an intrinsic ligand, or the extrinsic ligand, pyridine dissociates from the heme iron and the native Met80 reassociates. Thus, only one peak (P1′, corresponding to the reoxidation of native cyt c) is observed as the scan is reversed. If, however, the scan rate is comparable to or faster than the time scale of these rearrangements, the transient species are observed. This proposition is supported by the appearance of the counterparts of oxidation peaks P2′ and P3′ during the reverse scan at high scan rates in both experimental and simulated CVs.

**Acknowledgment.** Portions of this work were funded by the National Science Foundation under Grant No. DMR-0099843, and by the Office of Naval Research, under Grant No. ONR N0014-1-1-0239, and the National Institute of Health, under Grant No. GM 62958-01. The authors gratefully acknowledge helpful, critical commentary by Harry Gray, Pernilla Wittung-Stafshede, Paola Turano, and Ivano Bertini.

**Supporting Information Available:** UV−vis spectra of cyt c in a variety of conditions (Figure 1-S). Plots of formal potential $E^{\circ\prime}$ and apparent heterogeneous electron-transfer rate $k_s$ of the native form of cyt c verses the concentration of pyridine (Figure 2-S); Two tables for details of UV−vis and CD spectra for different species. This material is available free of charge via the Internet at http://pubs.acs.org.

## References and Notes


(1) Nelson, D. L.; Cox, M. M. *Lehninger Principles of Biochemistry*; Worth Publishers: New York, 2000.

(2) Kennedy, M. L.; Gibney, B. R. *Curr. Opin. Struct. Biol.* **2001**, *11*, 485−490.

(3) Benson, D. E.; Wisz, M. S.; Hellinga, H. W. *Curr. Opin. Biotech.* **1998**, *9*, 370−376.

(4) Gilardi, G.; Fantuzzi, A.; Sadeghi, S. J. *Curr. Opin. Struct. Biol.* **2001**, *11*, 491−499.

(5) Moore, G. R.; Pettigrew, G. W. *Cytochromes c, Evolutionary, Structural and Physicochemical Aspects*; Springer-Verlag: Berlin, 1990.

(6) Pettigrew, G. W.; Moore, G. R. *Cytochromes c, Biological Aspects*; Springer-Verlag: Berlin, 1987.

(7) Michel, B.; Proudfoot, A. E.; Wallace, C. J.; Bosshard, H. R. *Biochemistry* **1989**, *28*, 456−462.

(8) Cullison, J. K.; Hawkridge, F. M.; Nakashima, N.; Yoshikaw, S. *Langmuir* **1994**, *10*, 877−882.

(9) Haas, A. S.; Pilloud, D. J.; Reddy, K. S.; Babcock, G. T.; Moser, C. C.; Blasie, J. K., Dutton, P. L. *J. Phys. Chem. B* **2001**, *105*, 11 351−11 362.

(10) Yeh, S. R.; Takahashi, S.; Fan, B.; Rousseau, D. L. *Nature Struct. Biol.* **1997**, *4*, 51−56.

(11) Arcovito, A.; Gianni, S.; Brunori, M.; Travaglini-Allocatelli, C.; Bellelli, A. *J. Biol. Chem.* **2001**, *276*, 41 073−41 078.

(12) Telford, J. R.; Wittung-Stafshede P.; Gray H. B.; Winkler, J. R. *Acc. Chem. Res.* **1998**, *31*, 755−763.

(13) Chottard, G.; Michelon, M.; Herve, M.; Herve, G. *Biochim. Biophys. Acta* **1987**, *916*, 402−410.

(14) Hildebrandt, P. *Biochim. Biophys. Acta* **1990**, *1040*, 175−176.

(15) Bixler, J.; Bakker, G.; McLendon, G. *J. Am. Chem. Soc.* **1992**, *114*, 6938−6939.

(16) Pascher, T.; Chesick, J. P.; Winkler, J. R.; Gray, H. B. *Science* **1996**, *271*, 1558−1560.

(17) Williams, P. A.; Fulop, V.; Garman, E. F.; Saunders: N. F. W.; Ferguson, S. J.; Hajdu, J. *Nature* **1997**, *389*, 406−412.

(18) Poulos, T. L. *Nature Struct. Biol.* **1996**, *3*, 401−403.

(19) Bushnell, G. W.; Louie, G. V.; Brayer, G. D. *J. Mol. Biol.* **1990**, *214*, 585−595.

(20) Brennan, L.; Turner, D. L. *Biochim. Biophys. Acta* **1997**, *1342*, 1−12.

(21) Ma, D.; Lu, J.; Tang, W. *Biochim. Biophys. Acta* **1998**, *1384*, 32−42.

(22) Banci, L.; Bertini, I.; Spyroulias, G. A.; Turano, P. *Eur. J. Inorg. Chem.* **1998**, *1*, 583−591.

(23) Shao, W.; Tang, W. *Spectroscopy Lett.* **1994**, *27*, 763−773.

(24) Liu, G.; Chen, Y.; Tang, W. *J. Chem. Soc., Dalton Trans.* **1997**, 795−801.

(25) Elove, G. A.; Bhuyan, A. K.; Roder, H. *Biochemistry* **1994**, *33*, 6925−6935.

(26) Hildebrandt, P.; Vanhecke, F.; Buse, G.; Soulimane, T.; Mauk, A. G. *Biochemistry* **1993**, *32*, 10 912−10 922.

(27) Lu, J.; Ma, D.; Hu, J.; Tang, W.; Zhu, D. *J. Chem. Soc., Dalton Trans.* **1998**, 2267−2273.

(28) Yamamoto, H.; Liu, H.; Waldeck, H. *Chem. Commun.* **2001**, 1032−1033.

(29) Smith, M.; McLendon, G. *J. Am. Chem. Soc.* **1981**, *103*, 4912−4921.

(30) Shao, W.; Yao, Y.; Liu, G.; Tang, W. *Inorg. Chem.* **1993**, *32*, 6112−6114.

(31) Theorell, H.; Akesson, A. *J. Am. Chem. Soc.* **1941**, *63*, 1804−1811.

(32) Hildebrandt, P.; Heimburg, T.; Marsh, D. *Eur. Biophys. J.* **1990**, *18*, 193−201.

(33) Nelson, C. J.; Bowler, B. E. *Biochemistry* **2000**, *39*, 13 584−13 594.

(34) Dopner, S.; Hildebrandt, P.; Rosell, F. I.; Mauk, A. G. *J. Am. Chem. Soc.* **1998**, *120*, 11 246−11 255.

(35) Rosell, F. I.; Ferrer, J. C.; Mauk, A. G. *J. Am. Chem. Soc.* **1998**, *120*, 11 234−11 245.

(36) Barker, P. D.; Mauk, A. G. *J. Am. Chem. Soc.* **1992**, *114*, 3619−3624.

(37) Hong, X. L.; Dixon, D. W. *FEBS Lett.* **1989**, *246*, 105−108.

(38) Greenwood, C.; Palmer, G. *J. Biol. Chem.* **1965**, *240*, 3660−3663.

(39) Pecht, I.; Faraggi, M. *Proc. Natl. Acad. Sci. U.S.A.* **1972**, *69*, 902−906.

(40) Wilson, M. T.; Greenwood, C. *Eur. J. Biochem.* **1971**, *22*, 11−18.

(41) Ambundo, E. A.; Deydier, M. V.; Grall, A. J.; Aguera-Vega, N.; Dressel, L. T.; Cooper, T. H.; Heeg, M. J.; Ochrymowycz, L. A.; Rorabacher, D. B. *Inorg. Chem.* **1999**, *38*, 4233−4242.

(42) Yu, Q.; Salhi, C. A.; Ambundo, E. A.; Heeg, M. J.; Ochrymowycz, L. A.; Rorabacher, D. B. *J. Am. Chem. Soc.* **2001**, *123*, 5720−5729.

(43) Hirst, J. Duff, J. L. C., Jameson, G. N. L.; Kemper, M. A.; Burgess, B. K.; Armstrong, F. A. *J. Am. Chem. Soc.* **1998**, *120*, 7085−7094.

(44) Myer, Y. P. *Methods Enzymol.* **1978**, *LIV*, 249−285.

(45) Kamiyama, T.; Sadahide, Y.; Nogusa, Y.; Gekko, K. *Biochim. Biophys. Acta* **1999**, *1434*, 44−57.

(46) Wittung-Stafshede, P. *Biochim. Biophys. Acta* **1998**, *1382*, 324−332.

(47) Blauer, G.; Sreerama, N.; Woody, R. *Biochemistry* **1993**, *32*, 6674−6679.

(48) Tuominen, E. K. J.; Zhu, K.; Wallace, C. J. A.; Clark-Lewis, I.; Craig, D. B.; Rytomaa, M.; Kinnunen, P. K. J. *J. Biol. Chem.* **2001**, *276*, 19 356−19 362.

(49) Vanderkooi, J. M.; Erecinska, M. *Eur. J. Biochem.* **1975**, *60*, 199−120.

(50) Bhuyan, A. K.; Udgaonkar, J. B. *J. Mol. Biol.* **2001**, *312*, 1135−1160.

(51) Chan, C.; Hu, Y.; Takahashi, S.; Rousseau, D. L.; Eaton, W. A.; Hofrichter, J. *Proc. Natl. Acad. Sci. U.S.A.* **1997**, *94*, 1779−1784.

(52) Santucci, R.; Ascoli, F. *J. Inorg. Biochem.* **1997**, *68*, 211−214.

(53) Das, T. K.; Mazumdar, S.; Mitra, S. *Eur. J. Biochem.* **1998**, *254*, 662−670.

(54) Feinberg, B. A.; Liu, X.; Ryan, M. D.; Schejter, A.; Zhang, C. and Margoliash, E. *Biochemistry* **1998**, *37*, 13 091−13 101.

(55) Battistuzzi, G.; Borsari, M.; Loschi, L.; Righi, F.; Sola, M. *J. Am. Chem. Soc.* **1999**, *121*, 501−506.

(56) Borsari, M.; Sola M.; Francia, F. *Biochemistry* **1997**, *36*, 16 247−16 258.

(57) Ferri, T.; Poscia, A.; Ascoli, F.; Santucci, R. *Biochim. Biophys. Acta* **1996**, *1298*, 102−108.

(58) Pineda, T.; Sevilla, J. M.; Roman, A. J.; Blazquez, M. *Biochim. Biophys. Acta* **1997**, *1343*, 227−234.

(59) Seetharaman, R.; White S. P.; Rivera, M. *Biochemistry* **1996**, *35*, 12 455−12 463.

(60) Burrows, A. L.; Guo, L. H.; Hill, H. A. O.; McLendon, G.; Sherman, F. *Eur. J. Biochem.* **1991**, *202*, 543−549.

(61) Fan, C.; Chen, X.; Li, G.; Zhu, J.; Zhu, D.; Scheer, H. *Phys. Chem. Chem. Phys.* **2000**, *2*, 4409−4413.

(62) Hirota, S.; Endo, M.; Hayamizu, K.; Tsukazaki, T.; Takabe, T.; Kohzuma T.; Yamauchi, O. *J. Am. Chem. Soc.* **1999**, *121*, 849−855.

(63) King, B. C.; Hawkridge, F. M.; Hoffman, B. M. *J. Am. Chem. Soc.* **1992**, *114*, 10 603−10 608.

(64) Battistuzzi, G.; Borsari, M.; Dallari, D.; Lancellotti, I.; Sola, M. *Eur. J. Biochem.* **1996**, *241*, 208−214.

(65) Bard, A. J.; Faulkner, L. R. *Electrochemical Methods*, 2nd ed.; John Willey & Sons: New York, 2001.

(66) Nicholson, R. S. *Anal. Chem.* **1965**, *37*, 1351−1355.

(67) Sivakolundu, S. G.; Mabrouk, P. A. *J. Am. Chem. Soc.* **2000**, *122*, 1513−1521.

(68) Marques, H. M.; Cukrowski, I.; Vashi, P. R. *J. Chem. Soc., Dalton Trans.* **2000**, 1335−1342.

(69) Bruschi, M.; Woudstra, M.; Guigliarelli, B.; Asso, M.; Lojou, E.; Petillot, Y.; Abergel, C. *Biochemistry* **1997**, *36*, 10 601−10 608.

(70) Reid, L. S.; Taniguchi, V. T.; Gray, H. B.; Mauk, A. G. *J. Am. Chem. Soc.* **1982**, *104*, 7516−7519.

(71) Hamada, D.; Kidokoro, S.; Fukada, H.; Takahashi, K.; Goto, Y. *Proc. Natl. Acad. Sci. U.S.A.* **1994**, *91*, 10 325−10 329.

(72) Feng, M.; Tachikawa, H. *J. Am. Chem. Soc.* **2001**, *123*, 3013−3020.

(73) Schejter, A.; Aviram, I. *Biochemistry* **1969**, *8*, 149−153.

(74) Duah-Williams, L.; Hawkridge, F. M. *J. Electroanal. Chem.* **1999**, *466*, 177−186.

(75) Lambeth, D. O.; Campbell, K. L.; Zand, R.; Palmer, G. *J. Biol. Chem.* **1973**, *248*, 8130−8136.

(76) Abbruzzetti, S.; Viappiani, C.; Small, J. R.; Libertini, L. J.; Small, E. W. *J. Am. Chem. Soc.* **2001**, *123*, 6649−6653.

(77) Telford, J. R.; Tezcan, F. A.; Gray H. B. Winkler, J. R. *Biochemistry* **1999**, *38*, 1944−1949.